European Journal of Pharmacology 810 (2017) 149–155

Contents lists available at ScienceDirect

European Journal of Pharmacology

journal homepage: www.elsevier.com/locate/ejphar

Molecular and cellular pharmacology

Methyl (E)-(3-(3,4-dihydroxyphenyl)acryloyl)tryptophanate can suppress MCP-1 expression by inhibiting p38 MAP kinase and NF-κB in LPS-stimulated differentiated THP-1 cells

Jae B. Park*, Thomas T.Y. Wang

Diet, Genomics, and Immunology Laboratory, BHNRC, ARS, USDA, Bldg. 307C, Rm. 131, Beltsville, MD 20705, United States

ARTICLE INFO

Keywords:
Methyl (E)-(3-(3,4-dihydroxyphenyl)acryloyl) tryptophanate (MHAT)
Monocyte chemotactic protein-1 (MCP-1)
p38
ATF-2
NF-κB
THP-1

ABSTRACT

Methyl (E)-(3-(3,4-dihydroxyphenyl)acryloyl)tryptophanate (MHAT) is an O-methyl ester of javamide-II showing strong anti-inflammatory activity. Therefore, in this study, MHAT was chemically synthesized, and its effects on p38 MAP kinase, NF-κB, and monocyte chemotactic factor-1 (MCP-1) expression were investigated in LPS-stimulated differentiated THP-1 cells. MHAT inhibited p38 MAP kinase with an IC_{50} of 12 μM, and the inhibition was supported by an *in silico* model showing that its binding to p38 MAP kinase was stronger than that of SB203580. At the concentration of 20 μM, the p38 inhibition reduced ATF-2 phosphorylation by 55% ($P < 0.05$). Additionally, MHAT inhibited NF-κB (p65) phosphorylation by 30% ($P < 0.05$) at the same concentration, suggesting that MHAT was able to reduce NF-κB transcriptional activity. This supposition was confirmed by the NF-κB reporter assay, demonstrating that MHAT (20 μM) could suppress NF-κB transcriptional activity by 29% ($P < 0.05$) in the NF-κB reporter (Luc)-HEK293 cell line. As expected, the treatment with MHAT (5–40 μM) significantly inhibited MCP-1 mRNA expression by 9–73% ($P < 0.05$) and the production of MCP-1 protein by 10–70% ($P < 0.05$) in the THP-1 cells. Furthermore, MHAT was found to inhibit RANTES expression as well in the same THP-1 cells, supporting its purported inhibition of p38 MAP kinase and NF-κB. All these data suggest that MHAT is a potent compound that can inhibit MCP-1 production by suppressing p38 kinase/ATF-2 phosphorylation and NF-κB in the differentiated THP-1 cells.

1. Introduction

Monocyte chemotactic factor-1 (MCP-1) is a small but potent chemotactic factor belonging to the subfamily of CC chemokines (Deshmane et al., 2009; Leonard and Yoshimura, 1990). Its expression is reported to be ubiquitous in many different cell types and is often up-regulated by various stimuli including lipopolysaccharide (LPS), IL-1, TNF-alpha, and 2-O-tetradecanoylphorbol 13-acetate (TPA) (Kunkel et al., 1991; Martin et al., 1997). Because MCP-1 has a strong chemotactic activity on inflammatory cells, it can recruit blood monocytes into the vessel wall, thereby leading to systemic vascular inflammation commonly observed in cardiovascular disease (CVD) and other diseases (Fox and Kahn, 2005; Christodoulidis et al., 2014; Lin et al., 2014; Ruster and Wolf, 2008). Although the regulation of MCP-1 expression is considered complex and cell-specific, p38 MAP kinase and NF-κB are considered major regulatory molecules in the production of MCP-1 in cells (Sutcliffe et al., 2009; Yang et al., 2014; Saklatvala, 2004; Lee et al., 1999). Therefore, the inhibition of these molecules has been suggested as an effective means for suppressing MCP-1 production (Sheryanna et al., 2007; Wong et al., 2005).

Methyl (E)-(3-(3,4-dihydroxyphenyl)acryloyl)tryptophanate (MHAT) is an O-methyl ester of javamide-II which is a phenolic amide found in coffee (Park, 2016). During the course of our study, MHAT was found to have stronger anti-inflammatory activity than the parent chemical javamide-II, speculating its potential to inhibit the expression of inflammation-related molecules including MCP-1 in cells. However, there is currently little information about the capability of MHAT to inhibit p38 MAP kinase, NF-κB and MCP-1 expression in monocytic/macrophage-like cells. Therefore, in this study, MHAT was synthesized, and its potential effect on the expression of MCP-1 was investigated in LPS-stimulated differentiated THP-1 cells by examining its effects on p38 MAP kinase/ATF-2 phosphorylation and NF-κB

* Corresponding author.
E-mail address: jae.park@ars.usda.gov (J.B. Park).

http://dx.doi.org/10.1016/j.ejphar.2017.07.006
Received 20 April 2017; Received in revised form 23 June 2017; Accepted 3 July 2017
Available online 06 July 2017

phosphorylation/transcriptional activity. Additionally, the potential effect of MHAT on RANTES was investigated in the same cells because p38 MAP kinase and NF-κB are also significantly involved in the production of RANTES in the cells (Wong et al., 2005).

2. Materials and methods

2.1. Materials

Tryptophan, cinnamic acid, dichloromethane, N,N-dimethylformamide, SB203580, Phorbol 12-myristate 13-acetate (PMA) and other chemicals were purchased from Sigma Chemical Co. (St. Louis, MO). THP-1 cells were purchased from ATCC (Manassas, VA). Alpha-tubulin (Catalog no. 2144), ATF-2 (Catalog no. 9226) and phospho-ATF-2 (Catalog no. 5112) antibodies were purchased from Cell Signaling (Danvers, MA, USA)

2.2. Chemical synthesis

The synthesis of MHAT was performed using a method described previously (Park, 2012). Briefly, caffeic acid was dissolved in dimethyl sulfoxide (DMSO) and converted to the symmetrical anhydride with 1,3-diisopropylcarbodiimide (DIC). Next, tryptophan-O-methyl was synthesized using tryptophan and methanol and added to the reaction mixture. The reaction mixture was incubated at room temperature with a gentle stirring for 12 h. The synthesized products were recovered and purified by HPLC (Waters, Milford, MA) as described previously (Park, 2012). MHAT was prepared in ethanol for use in experiments.

2.3. p38 MAP kinase assay

Measurement of p38 MAP kinase activity was carried out by using CycLex p38 assay/inhibitor screening kit-1 (MBL International, Woburn, MA), which uses anti-phospho-ATF2 Thr71 polyclonal antibody (PPT-08) and peroxidase coupled anti-rabbit IgG antibody as the reporter molecule in a 96-well ELISA format. The assay method involves the incubation of the p38 sample with the substrate and the tested compound in the presence of Mn2+ and ATP, and the assay was carried out according to the manufacturer's protocol.

2.4. Molecular docking

Molecular docking studies were performed using the algorithm-based docking program ICM-pro (MolSoft, San Diego, CA). The proposed binding to the active site pocket of p38 MAP kinase was determined by the best ranked scoring function of ICM-pro, which also represents the conformational structures with the most favorable free binding energy ($\Delta G_{binding}$).

2.5. Cell culture

THP-1 cells were purchased from the ATCC (Manassas, VA). Cells were grown in RPMI 1640 medium with L-glutamine containing 10% FBS, 100 units/ml penicillin, and 100 units/ml streptomycin. THP-1 cells were maintained at 37 °C in a humidified atmosphere of 5% CO_2. THP-1 cells were induced to differentiate into macrophages by incubation with PMA (25 ng/ml) for 48 h. The differentiated cells (2×10^6 cells/well) were treated with several concentrations of MHAT (0–40 μM) followed by the treatment with LPS (10 ng/ml) (Huang et al., 2012) and incubated for specified times at each experiment. Also, the media were saved for quantifying MCP-1 and RANTES proteins.

2.6. Cell growth assay

The differentiated THP-1 cells (5×10^5 cells/well) plated in 6-well plates were treated with 0, 5, 20, and 40 μM of MHAT for 10 min followed by LPS treatment (10 ng/ml) for 4 h. Cell growth was analyzed using the sulforhodamine B assay as described previously (Vichai et al., 2006).

2.7. Western blot of phospho-ATF-2

For the Western blot of phospho-ATF-2, the samples were prepared using the PMA-differentiated THP-1 cells treated with MHAT (0, 20, 40 μM) followed by the treatment with LPS (10 ng/ml) for 0.5 h. The Western blots were generated using Novex 4–12% Tris-Glycine Mini Gels and a XCell II™ Blot Module kit (Life Technologies, Cambridge, MA, USA) with ATF-2 (Catalog no. 9226), phospho-ATF-2 (Catalog no. 5112) and alpha-tubulin (Catalog no. 2144) antibodies (Cell Signaling, Danvers, MA, USA). LI-COR IRDye 800CW anti-rabbit IgG (Catalog no. 926-32213) (Lincoln, NE, USA) was used as a second antibody. For the blot, the amounts of protein in the samples were determined using the Bio-Rad protein assay kit (Hercules, CA, USA), and the protein bands in the Western blot were quantified using an Odyssey CLx imaging system (Lincoln, NE, USA).

2.8. Binding assay of NF-κB (p65)

The binding of NF-κB (p65) to its cognate element site was measured using the NF-κB (p65) Transcription Factor Assay kit according to the manufacturer's protocol (Cayman Chemical, Ann Arbor, Michigan). The NF-κB (human p65) transcription factor assay is a convenient and sensitive method for detecting specific transcription factor DNA binding activity in nuclear extracts. A specific double stranded DNA (dsDNA) sequence with the NF-κB response element is coated onto the wells of a 96-well plate. The nuclear extracts with NF-κB (p65) were prepared using differentiated THP-1 cells treated with MHAT (0, 1, 10, 20 μM) followed by LPS treatment (10 ng/ml) for 10 h. The samples were incubated overnight at 4 °C in the wells, allowing the NF-κB (p65) in the extracts to bind to its cognate site. The bound NF-κB (p65) transcriptional factors were detected using a specific primary antibody against NF-κB (p65) followed by a secondary antibody conjugated to horseradish peroxidase (HRP), which provides a sensitive colorimetric readout at 450 nm.

2.9. NF-κB reporter assay

The NF-κB signal transduction pathway was monitored using the NF-κB reporter (Luc)-HEK293 cell line (Signosis, Inc., Santa Clara, CA), which contains a firefly luciferase gene driven by four copies of the NF-κB response element located upstream of the minimal TATA promoter. For the study, the HEK293 cells were pre-incubated with MHAT (0, 10, 20, 40 μM) for 1 h followed by treatment with TNF-alpha (10 ng/ml). The treatment led to the binding of endogenous NF-kB transcription factors to the DNA response elements and induced transcription of the luciferase reporter gene, which monitors NF-κB signal transduction. Luciferase activity was measured using a microplate luminometer (Berthold Technologies, Bad Wildbad, Germany).

2.10. RNA isolation and real time RT-PCR quantitation of COX-2 and MCP-1 mRNA

Total RNA was isolated from the differentiated THP-1 cells treated with various concentrations of MHAT (0, 5, 20 and 40 μM) followed by LPS treatment (10 ng/ml) for 4 h using TRIzol™ reagent (Invitrogen, Carlsbad, CA). Complementary DNA (cDNA) was synthesized from 1 μg of the total RNA using the AffinityScript Multiple Temperature cDNA Synthesis Kit (Agilent Technologies, Inc., Santa Clara, CA) according to the manufacturer's protocol. Real time semi-quantitative PCR was carried out using the TaqMan® Fast Universal PCR Master Mix (2X) (Applied Biosystems, Foster City, CA) and a ViiA7 Real-Time PCR Detection System (Applied Biosystems, Foster City, CA) following

the manufacturer's protocol. Human TaqMan probes and primers were purchased from Applied Biosystems (Foster City, CA) using inventoried TaqMan gene expression assays: TATA box binding protein (assay ID: Hs00427620_m1), MCP-1/CCL2 (assay ID: Hs00234140_m1) (Takahashi et al., 2007) and COX-2/PTGS2 (assay ID: Hs00153133_m1) (For more information; http://www.thermofisher.com).

2.11. Determination of MCP-1 and RANTES

MCP-1 and RANTES levels in the media of the differentiated THP-1 cells treated with various concentrations of MHAT (0–40 μM) followed by LPS treatment (10 ng/ml) for 9 h were determined using the Human Quantikine MCP-1 Elisa kit and the RANTES Elisa kit from R & D systems (Minneapolis, MN) according to the manufacturer's protocol.

2.12. Statistical analysis

All statistical analyses were performed with SigmaPlot 11.0 (Chicago, IL). The P value was calculated using one-way ANOVA with the Holm-Sidak method, and $P < 0.05$ was considered as statistically significant. Data points in all figures were represented as the means ± S.D.

3. Results

MHAT (methyl (E)-(3-(3,4-dihydroxyphenyl)acryloyl)tryptophanate) (Fig. 1) was synthesized using the method described in Section 2,and the product was purified by HPLC (Waters, Milford, MA) as described previously (Park, 2012). To confirm the identities of the synthesized products, the sample was analyzed using NMR spectroscopic methods as described in Section 2, (see Supplementary data for NMR data). Based on the NMR data, the structure of the product was determined as that of methyl (E)-(3-(3,4-dihydroxyphenyl)acryloyl)tryptophanate (Fig. 1). The p38 MAP kinase pathway is critically involved in the production of several inflammatory chemokines including MCP-1 (Waas et al., 2001; Liang et al., 2015; Genovese et al., 2011; MacNee et al., 2013; Yang et al., 2014; Lomas et al., 2012; Bison et al., 2011; Elkhawad et al., 2012). Also, several studies suggested that the inhibition of p38 MAP kinase often led to the suppression of MCP-1 expression in humans (Genovese et al., 2011; MacNee et al., 2013; Lomas et al., 2012; Bison et al., 2011; Elkhawad et al., 2012). Therefore, we investigated the potential effects of MHAT on p38 MAP kinase activity to find a candidate compound for inhibiting MCP-1 expression. As shown in Fig. 2, MHAT was able to inhibit p38 MAP kinase significantly, and the calculated IC_{50} was approximately 12 μM. Since MHAT showed relatively strong p38 MAP kinase inhibition, a qualitative molecular docking was performed with MHAT against available p38 MAP kinase complexes to confirm the observed p38 MAP kinase inhibition. This docking study was performed using the algorithm-based docking program ICM-pro as described in Section 2. The docking experiments were performed with MHAT and SB203580 (a known p38 MAP kinase inhibitor) using the experimentally determined crystal structures of p38 MAP kinase complexes (14 complexes, Table 1). Briefly, the p38 MAP kinase complex was divided into ligand and protein, and the ligands (MHAT and SB203580) were docked into the protein complexes. The docked complexes with the lowest energy and outcome scoring values were compared (Table 1). In Fig. 3, the lowest energy position of MHAT docked into the p38 MAP kinase protein (PDB_ID; 3HV5) was presented as a putative binding mode. Overall, MHAT exhibited higher scores than those of SB203580, suggesting that MHAT may inhibit p38 MAP kinase.

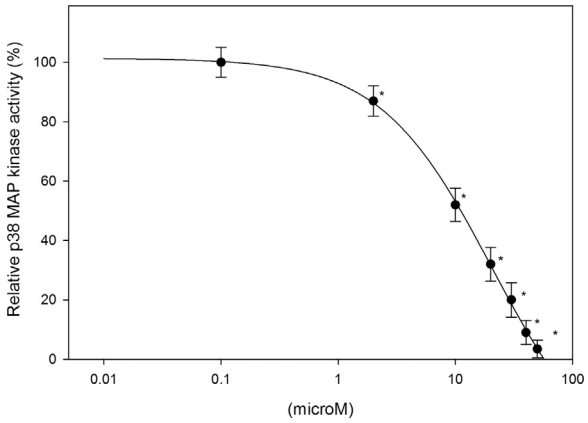

Fig. 2. The inhibition of p38 MAP kinase and determination of IC_{50}. The inhibition of p38 by MHAT was determined at the concentrations between 0 and 50μM. Data points are shown as the means ± S.D. (n = 4). The P value was calculated using one-way ANOVA with the Holm-Sidak method, and the asterisks (*) denote significant differences ($P < 0.05$) from the vehicle control.

Often, cell death induces massive gene deregulation, which could complicate efforts to delineate specific gene regulation after treatment with inhibitors. Therefore, we performed a cell growth assay to ensure that MHAT is not cytotoxic to the differentiated THP-1 cells at the concentrations used in this experiment (Fig. 4). At concentrations between 0 and 40 μM, MHAT was found to inhibit p38 MAP kinase greatly but was considered non-cytotoxic (Fig. 4), although a slight decrease in cell attachment was found at 40 μM. In accordance with this result, other cell death assays (e.g., MTT, LDH) also showed no significant cell death (data not shown here). Next, the effect of MHAT on the phosphorylation of ATF-2 was investigated because the activation of p38 MAP kinase played an important role in the expression of MCP-1 (van Dam and Castellazzi, 2001) and because p38 MAP kinase can modulate transcriptional up-regulation of MCP-1 by the phosphorylation of several transcription factors such as activating transcription factor-2 (ATF-2) (van Dam and Castellazzi, 2001). As shown in Fig. 5, phosphorylated ATF-2 was significantly reduced in the differentiated THP-1 cells by the treatment with MHAT (20 and 40 μM). These data

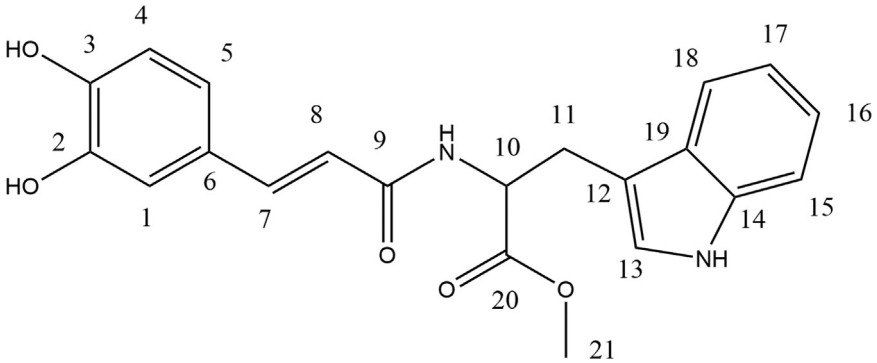

Fig. 1. Chemical structure of MHAT. The chemical synthesis was performed as described in Section 2. The chemical structure was verified using NMR.

Table 1
p38 MAPK docking scores of MHAT and SB203580. Docking scores and energy values were obtained using a docking program ICM-pro as described in Section 2. Average data represents the means ± S.D. (n = 14).

MHAT			SB203580	
p38 (PDB_ID)	Score	ΔE (Kcal/mol)	Score	ΔE (Kcal/mol)
3HV5	− 39.2	− 47.1	− 34.4	− 42.3
1W83	− 31.7	− 39.4	− 24.7	− 37.1
1W84	− 28.4	− 37.5	− 22.3	− 32.1
2PUU	− 25.9	− 35.4	− 21.5	− 29.5
3BV2	− 27.8	− 38.3	− 5.9	− 12.2
3GC9	− 32.6	− 39.1	− 24.1	− 36.3
3GCU	− 36.7	− 46.6	− 24.3	− 35.5
3D7Z	− 29.7	− 38.8	− 16.0	− 17.0
3DS6	− 31.2	− 44.2	− 21.8	− 32.9
3QUD	− 18.4	− 29.4	− 16.0	− 27.6
3L8S	− 27.2	− 39.7	− 19.3	− 30.2
4R3C	− 26.1	− 38.2	− 17.0	− 30.5
4KIP	− 27.9	− 37.4	− 16.0	− 25.1
4DLI	− 28.7	− 36.7	− 25.3	− 34.5
Average	**− 29.3 ± 4.9**[a]	**− 39.1 ± 4.5**[b]	**− 20.6.1 ± 6.5**	**− 30.2 ± 7.9**

[a] P < 0.05 MHAT vs SB203580 Score (paired *t*-test; t = 6.482 df = 13).
[b] P < 0.05 MHAT vs SB203580 ΔE (paired *t*-test; t = 4.552 df = 13).

suggest that MHAT treatment could suppress the phosphorylation of ATF-2 possibly via inhibiting p38 MAP kinase.

The NF-κB/Rel family of transcription factors is comprised of several structurally related proteins that form homodimers and heterodimers (e.g., p50/p105, p52/p100, and RelA/p65) (Tai et al., 2013; Perkins, 2007). Some studies indicated that LPS treatment could lead to the binding of p65/p65, c-Rel/p65 and p50/p65 to their cognate DNA sites, which eventually increased MCP-1 mRNA in THP-1 cells (Tai et al., 2013). Therefore, we prepared the nuclear extracts of the differentiated THP-1 cells treated with MHAT (0, 1, 20, 40 μM) as described in Section 2 and investigated whether the binding of nuclear NF-κB p65 to the NF-κB response element could be affected by the treatment with MHAT. As shown in Fig. 6, MHAT treatment blocked the binding of NF-κB (p65) to the NF-κB response element when compared to the control, suggesting that the treatment could inhibit NF-κB (p65) phosphorylation. The reduction of NF-κB transcriptional activity by MHAT was also investigated using the NF-κB reporter (Luc)-HEK293 cell line, which is designed for monitoring nuclear factor Kappa B (NF-κB) signal transduction pathways (Pessara and Koch, 1990). As shown in Fig. 7, MHAT treatment (20 and 40 μM) lowered relative luminescent signals from the reporter gene by 28–40% (P < 0.05). Furthermore, potential effect of MHAT on COX-2 mRNA expression was investigated, because NF-κB is critically involved in the expression of COX-2 mRNA (Surh et al., 2001; Jobin et al., 1998). As expected, MHAT significantly inhibited COX-2 mRNA expression (Fig. 8), suggesting that MHAT could inhibit the transcriptional activity of NF-κB stimulated by LPS.

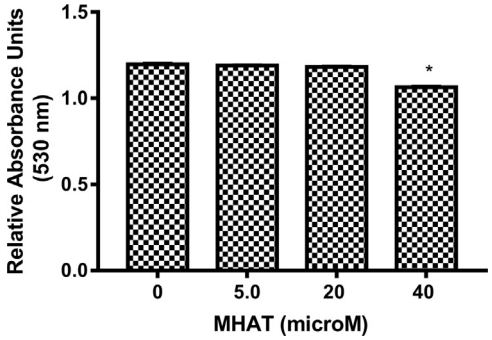

Fig. 4. Effects of MHAT on the growth of differentiated THP-1 cells. Cells were treated with several concentrations of MHAT (0, 5, 20, 40 μM), and cell growth was determined at 4 h. Data are presented as the means ± S.D. (n = 3). The P value was calculated using one-way ANOVA with the Holm-Sidak method, and the asterisks (*) indicate statistically significant differences (P < 0.05) compared to the control.

Since MHAT was able to inhibit p38 MAP kinase, ATF-2 phosphorylation and NF-κB transcriptional activity, the dose-dependent effects of MHAT on the expression of MCP-1 mRNA were investigated in differentiated THP-1 cells as described in Section 2. As shown in Fig. 9,

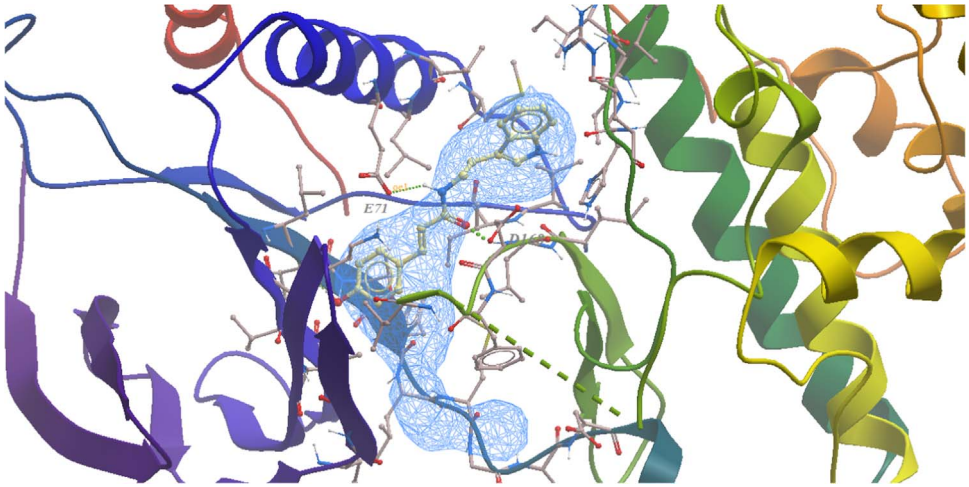

Fig. 3. *In silico* analysis of MHAT binding to p38. The MHAT in p38 complex (3HV5) is shown with two potential hydrogen bonds denoted by two green dots (E71) and (D168).

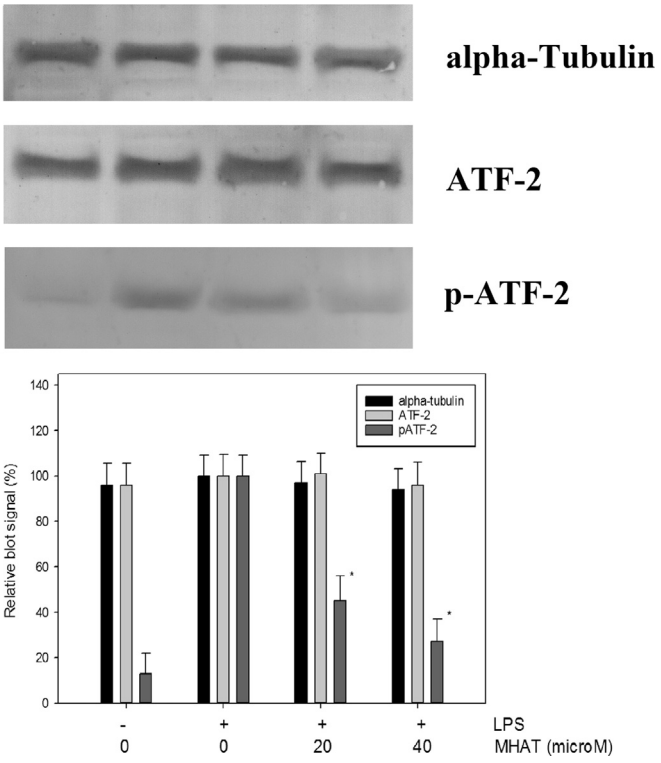

Fig. 5. Effects of MHAT on ATF-2 phosphorylation. The samples were prepared using differentiated THP-1 cells treated with MHAT (0, 20, 40 μM) followed by LPS treatment (0.01 μg/ml) for 0.5 h. For the phospho-ATF-2, ATF-2 control and alpha-tubulin blots, the data are presented as values of the means ± S.D. (n = 3) and each LPS data are presented as 100% relative blot signal. The P value was calculated using one-way ANOVA with the Holm-Sidak method, and the asterisks (*) indicate significant differences ($P < 0.05$) compared to the LPS control.

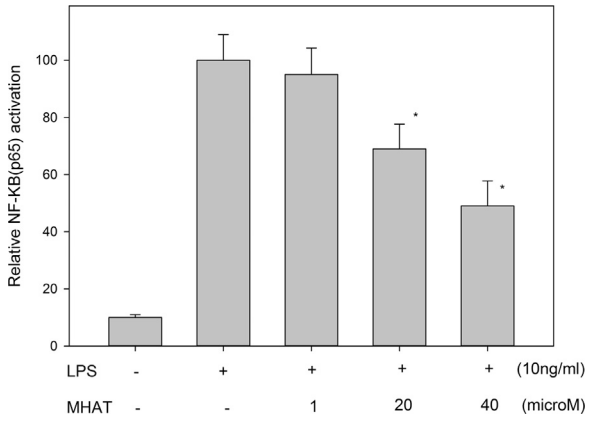

Fig. 6. Effects of MHAT on NF-κB (p65) phosphorylation. The samples were prepared using differentiated THP-1 cells treated with MHAT (0, 1, 20, 40 μM) followed by treatment with LPS (0.01 μg/ml) for 10 h. Data points represent the means ± S.D. (n = 4). The P value was calculated using one-way ANOVA with the Holm-Sidak method and the asterisks (*) denote significant differences ($P < 0.05$) for all groups (except group 2 vs. group 3, group vs. group 4, and group 4 vs. group 5).

the treatment with MHAT decreased MCP-1 mRNA expression in a dose-dependent manner. These data clearly suggest that MHAT can suppress MCP-1 mRNA expression significantly at the concentrations of 20 and 40 μM. Since MHAT could reduce the expression of MCP-1 mRNA, we investigated its effects on the expression of MCP-1 protein in the same THP-1 cells. As in previous experiments, the differentiated cells were treated with MHAT (0, 10, 20, 30, 40 μM) and followed by LPS treatment as described in Section 2. As expected, the MHAT treatment significantly inhibited the production of MCP-1 protein by 10–70% ($P < 0.05$) in the THP-1 cells (Fig. 10). Since SB203580 is a

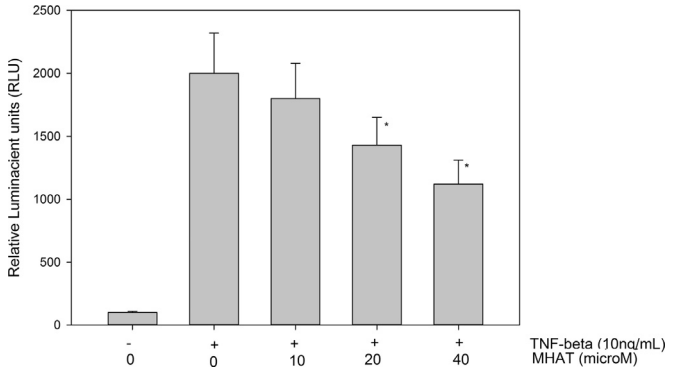

Fig. 7. Effects of MHAT on HEK293 cells containing the NF-κB reporter gene. The samples were prepared by treating HEK293 cells containing the NF-κB reporter gene with several concentrations of MHAT (0, 10, 20, 40 μM) followed by TNF-alpha (10 ng/ml) for 9 h. Data points represent the means ± S.D. (n = 4). The P value was calculated using one-way ANOVA with the Holm-Sidak method, and the asterisks (*) indicate significant differences ($P < 0.05$) compared to the control.

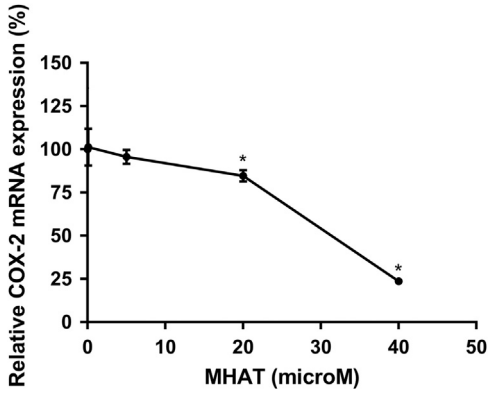

Fig. 8. Effects of MHAT on LPS-induction of COX-2 mRNA in differentiated THP-1 cells. The differentiated THP-1 cells were treated with 0, 5, 20 and 40 μM MHAT followed by treatment with LPS (0.01 μg/ml). RNA was isolated at 4 h, and gene expression of COX-2 was determined using real-time PCR. The percentage inhibition is expressed as the means ± S.D. (n = 3). Data were analyzed using one-way ANOVA with the Holm-Sidak method as described in Section 2. The asterisks (*) denote significant differences ($P < 0.05$) compared to the vehicle control.

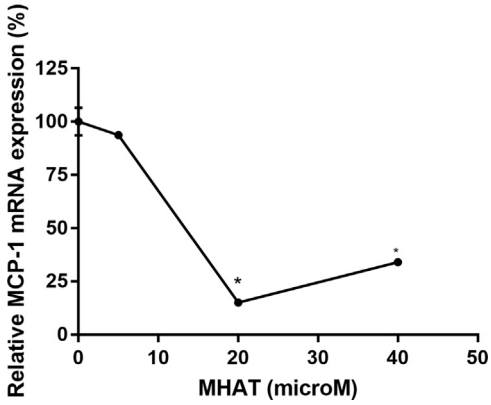

Fig. 9. Effects of MHAT on LPS-induction of MCP-1 mRNA in differentiated THP-1 cells. The differentiated THP-1 cells were treated with 0, 5, 20 and 40 μM MHAT followed by treatment with LPS (0.01 μg/ml). RNA was isolated at 4 h, and gene expression of MCP-1 was determined using real-time PCR. The percentage inhibition is expressed as the means ± S.D. (n = 3)(S.D. was too small to mark). Data were analyzed using one-way ANOVA with the Holm-Sidak method as described in Section 2. The asterisks (*) denote significant differences ($P < 0.05$) compared to the vehicle control.

well-known p38 inhibitor that can suppress LPS-induced MCP-1 expression (Perkins, 2007), the inhibitory effects of MHAT and SB203580 on the expression of MCP-1 protein were compared at 20

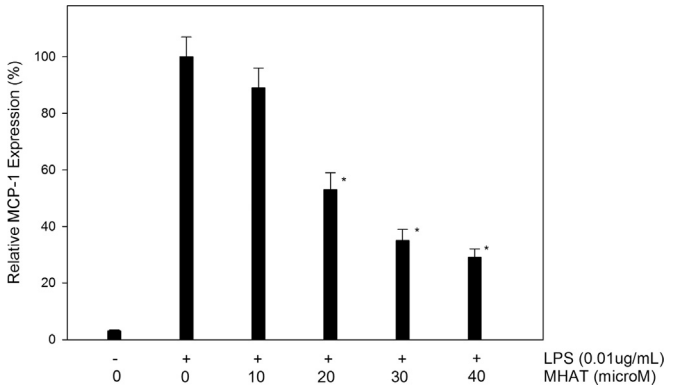

Fig. 10. Effects of MHAT on MCP-1 protein expression in differentiated THP-1 cells. The samples were prepared using differentiated THP-1 cells treated with MHAT (0, 10, 20, 30, 40 μM) followed by LPS treatment (0.01 μg/ml) for 9 h as described in Section 2. Data points represent the means ± S.D. (n = 5). The P value was calculated using one-way ANOVA with the Holm-Sidak method, and the asterisks (*) indicate significant differences ($P < 0.05$; $F(5, 24) = 259.5$) for all groups (except group 2 vs. group 3 and group 5 vs. group 6).

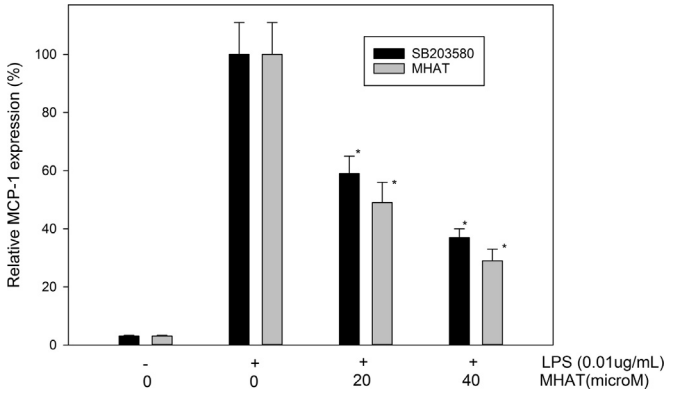

Fig. 11. Comparison of the effects of MHAT and SB203580 on MCP-1 protein expression in differentiated THP-1 cells. The samples were prepared using differentiated THP-1 cells treated with two concentrations of MHAT and SB203580 (20 and 40 μM) followed by treatment with LPS (0.01 μg/ml) for 9 h as described in Section 2. Data points represent the means ± S.D. (n = 4). The P value was calculated using one-way ANOVA with the Holm-Sidak method, and the asterisks (*) denote significant differences ($P < 0.05$; $F(3, 16) = 198.7$) for all groups.

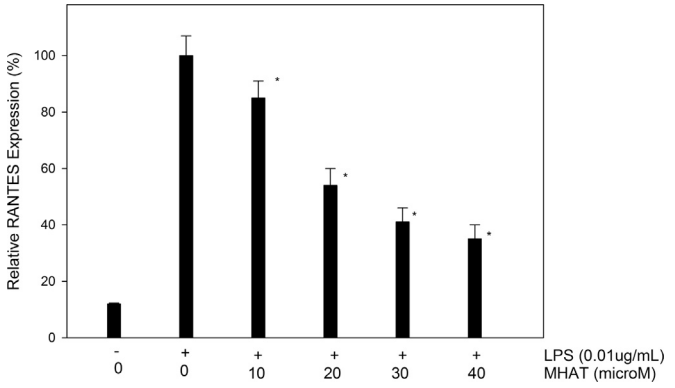

Fig. 12. Effects of MHAT on RANTES expression in differentiated THP-1 cells. The samples were prepared using differentiated THP-1 cells treated with MHAT (0, 10, 20, 30, 40 μM) followed by treatment with LPS (0.01 μg/ml) for 9 h as described in Section 2. Data points represent the means ± S.D. (n = 5). The P value was calculated using one-way ANOVA with the Holm-Sidak method, and the asterisks (*) denote significant differences ($P < 0.05$; $F(5, 24) = 188.3$) for all groups (except group 4 vs. group 5 and group 5 vs. group 6).

and 40 μM. As shown in Fig. 11, MHAT was found to be a marginally better inhibitor of MCP-1 protein than SB203580. To further substantiate the purported inhibition of p38 kinase and NF-κB, we investigated the effect of MHAT on another chemokine, RANTES, which is also regulated significantly by both p38 kinase and NF-κB (Hirano et al., 2003). As expected, MHAT treatment (10–40 μM) inhibited RANTES expression by 15–65% ($P < 0.05$) in the differentiated THP-1 cells (Fig. 12). These data suggest that MHAT can suppress p38 MAP kinase, ATF-2 phosphorylation, and NF-κB, thereby inhibiting MCP-1 and RANTES production in LPS-stimulated differentiated THP cells.

4. Discussion

In this study, MHAT was found to inhibit MCP-1 production in LPS-stimulated differentiated THP cells by inhibiting p38 kinase/ATF-2 phosphorylation as well as NF-κB. MCP-1 is a significant inflammatory chemokine involved in progressive chronic vascular/interstitial inflammation in CVD, chronic kidney disease and other diseases (Christodoulidis et al., 2014; Lin et al., 2014). There are several isoforms (p38α, β, γ and δ) of p38 MAP kinase that are activated by a variety of cellular stresses including osmotic shock, inflammatory cytokines, LPS, UV light and growth factors (Yang et al., 2014; Saklatvala, 2004; Lee et al., 1999; Sheryanna et al., 2007). Particularly, some p38 MAP kinase isoforms (α and β) play critical roles in the production of chemokines and cytokines (Lin et al., 2014; Ruster and Wolf, 2008; Yang et al., 2014; Takaishi et al., 2003). Interestingly, several p38 MAPK inhibitors have been demonstrated to inhibit the production of inflammatory cytokines/chemokines such as interleukin-1, TNF-alpha and MCP-1. Although the observed inhibitory effects are likely from the combined effects at the transcriptional and translational levels rather than the p38 MAPK pathway alone, several studies suggest that p38 MAPK inhibitors may be proficient in reducing plasma MCP-1 expression in humans (Liang et al., 2015; Genovese et al., 2011; MacNee et al., 2013), thereby providing protective effects in inflammatory cardiovascular disease (Lomas et al., 2012; Bison et al., 2011). Therefore, in this study, the potential effects of MHAT on MCP-1 expression were investigated in differentiated THP-1 cells in order to explore a candidate for MCP-1 inhibitor. As shown in Table 1, the docking data showed that the sum of ΔE value of MHAT binding (ΔE = − 39.1) was lower than that of the p38 inhibitor SB203580 (ΔE = − 31.7), suggesting that MHAT can bind to the putative binding site better than SB203580. Also, as shown in Fig. 3, the contours of the putative binding site were more accessible to MHAT in the tested p38 enzyme complex (3HV5) than SB203580 because MHAT has a less bulky structure than SB203580. As a consequence, the proposed two hydrogen bonds ((E71) and (D168) in Fig. 3) is very unlikely to be formed with SB203508 due to its structural conformation. However, in vitro p38 assay data showed that the IC_{50} of p38 MAP kinase inhibition by MHAT was approximately 12 μM, which showed that it was less effective than SB203580 (Fehr et al., 2015) and not in line with the docking data. Therefore, we reasonably thought that SB203580 may inhibit MCP-1 production stronger than MHAT in the cells. However, in differentiated THP-1 cells, the inhibition of MCP-1 protein production by MHAT was marginally better than that of SB203580, suggesting that MHAT may inhibit more than p38 MAP kinase with regard to MCP-1 inhibition. This inference was in fact supported by the finding that MHAT could inhibit NF-κB transcriptional activity. Like p38 MAP kinase, NF-κB is also significantly involved in the synthesis of MCP-1 in cells. The NF-κB transcription factors are composed of several proteins, which are present as homodimers and heterodimers (e.g., p50/p105, p52/p100, and RelA/p65) (Tai et al., 2013; Perkins, 2007). After the phosphorylation of I_KB by IKK, these transcription factors move into the nucleus and bind to their cognate binding elements on DNA, regulating the expression of target genes (Perkins, 2007). Some studies showed that LPS treatment could lead to the binding of p65/p65, c-

Rel/p65, and p50/p65 to their cognate DNA sites and initiate the expression of MCP-1 mRNA in cells (Tai et al., 2013). In this study, MHAT was clearly demonstrated to inhibit the phosphorylation of NF-κB (p65), thereby suppressing its transcriptional activity in the cells. These data suggest that the MHAT could suppress MCP-1 mRNA production in LPS-stimulated differentiated THP cells, probably by a concerted inhibition of p38 kinase/ATF-2 phosphorylation and NF-κB. Additionally, this purported p38 kinase and NF-κB inhibition was substantiated by the data that MHAT could inhibit the production of RANTES whose expression is significantly dependent on p38 kinase and NF-κB (Hirano et al., 2003). In summary, the data from this study showed that MHAT is a potential candidate compound to inhibit MCP-1 expression possibly via inhibiting p38 MAP kinase and NF-κB in the differentiated THP cells.

Conflict of interest statement

There are no disclosures to make about financial, consulting, and personal relationships linked to this paper.

Acknowledgements

This study was funded by the USDA (Project no. 8040-51000-057-00D).

Appendix A. Supporting information

Supplementary data associated with this article can be found in the online version at doi:10.1016/j.ejphar.2017.07.006.

References

Bison, S., Razzoli, M., Arban, R., Michielin, F., Bertani, S., Carboni, L., 2011. Effect of the p38 MAPK inhibitor SB-239063 on lipopolysaccharide-induced psychomotor retardation and peripheral biomarker alterations in rats. Eur. J. Pharmacol. 661, 49–56.

Christodoulidis, G., Vittorio, T.J., Fudim, M., Lerakis, S., Kosmas, C.E., 2014. Inflammation in coronary artery disease. Cardiol. Rev. 22, 279–288.

van Dam, H., Castellazzi, M., 2001. Distinct roles of Jun: Fos and Jun: ATF dimers in oncogenesis. Oncogene 20, 2453–2464.

Deshmane, S.L., Kremlev, S., Amini, S., Sawaya, B.E., 2009. Monocyte chemoattractant protein-1 (MCP-1): an overview. J. Interferon Cytokine Res. 29, 313–326.

Elkhawad, M., Rudd, J.H., Sarov-Blat, L., Cai, G., Wells, R., Davies, L.C., Collier, D.J., Marber, M.S., Choudhury, R.P., Fayad, Z.A., Tawakol, A., Gleeson, F.V., Lepore, J.J., Davis, B., Willette, R.N., Wilkinson, I.B., Sprecher, D.L., Cheriyan, J., 2012. Effects of p38 mitogen-activated protein kinase inhibition on vascular and systemic inflammation in patients with atherosclerosis. JACC Cardiovasc. Imaging 5, 911–922.

Fehr, S., Unger, A., Schaeffeler, E., Herrmann, S., Laufer, S., Schwab, M., Albrecht, W., 2015. Impact of p38 MAP kinase inhibitors on LPS-induced release of TNF-α in whole blood and primary cells from different species cell. Physiol. Biochem. 36, 2237–2249.

Fox, E.A., Kahn, S.R., 2005. The relationship between inflammation and venous thrombosis. A systematic review of clinical studies. Thromb. Haemost. 94, 362–365.

Genovese, M.C., Cohen, S.B., Wofsy, D., Weinblatt, M.E., Firestein, G.S., Brahn, E., Strand, V., Baker, D.G., Tong, S.E., 2011. A 24-week, randomized, double-blind, placebo-controlled, parallel group study of the efficacy of oral SCIO-469, a p38 mitogen-activated protein kinase inhibitor, in patients with active rheumatoid arthritis. J. Rheumatol. 38, 846–854.

Hirano, F., Komura, K., Fukawa, E., Makino, I., 2003. Tumor necrosis factor alpha (TNF-alpha)-induced RANTES chemokine expression via activation of NF-kappaB and p38 MAP kinase: roles of TNF-alpha in alcoholic liver diseases. J. Hepatol. 38, 483–489.

Huang, H.Q., Fletcher, A., Niu, Y.G., Wang, T.T., Yu, L.L., 2012. Characterization of lipopolysaccharide-stimulated cytokine expression in macrophages and monocytes. Inflamm. Res. 61, 1329–1338.

Jobin, C., Morteau, O., Han, D.S., Balfour Sartor, R., 1998. Specific NF-kappaB blockade selectively inhibits tumour necrosis factor-alpha-induced COX-2 but not constitutive COX-1 gene expression in HT-29 cells. Immunology 95, 537–543.

Kunkel, S.L., Standiford, T., Kasahara, K., Strieter, R.M., 1991. Stimulus specific induction of monocyte chemotactic protein-1 (MCP-1) gene expression. Adv. Exp. Med. Biol. 305, 65–71.

Lee, J.C., Kassis, S., Kumar, S., Badger, A., Adams, J.L., 1999. p38 mitogen-activated protein kinase inhibitors–mechanisms and therapeutic potentials. Pharmacol. Ther. 82, 389–397.

Leonard, E.J., Yoshimura, T., 1990. Human monocyte chemoattractant protein-1 (MCP-1). Immunol. Today 11, 97–101.

Liang, B., Wang, X., Zhang, N., Yang, H., Bai, R., Liu, M., Bian, Y., Xiao, C., Yang, Z., 2015. Angiotensin-(1-7) attenuates angiotensin II-induced ICAM-1, VCAM-1, and MCP-1 expression via the MAS receptor through suppression of P38 and NF-κB pathways in HUVECs. Cell. Physiol. Biochem. 35, 2472–2482.

Lin, J., Kakkar, V., Lu, X., 2014. Impact of MCP-1 in atherosclerosis. Curr. Pharm. Des. 20, 4580–4588.

Lomas, D.A., Lipson, D.A., Miller, B.E., Willits, L., Keene, O., Barnacle, H., Barnes, N.C., Tal-Singer, R., 2012. Losmapimod study investigators. An oral inhibitor of p38 MAP kinase reduces plasma fibrinogen in patients with chronic obstructive pulmonary disease. J. Clin. Pharmacol. 52, 416–424.

MacNee, W., Allan, R.J., Jones, I., De Salvo, M.C., Tan, L.F., 2013. Efficacy and safety of the oral p38 inhibitor PH-797804 in chronic obstructive pulmonary disease: a randomised clinical trial. Thorax 68, 738–745.

Martin, T., Cardarelli, P.M., Parry, G.C., Felts, K.A., Cobb, R.R., 1997. Cytokine induction of monocyte chemoattractant protein-1 gene expression in human endothelial cells depends on the cooperative action of NF-kappa B and AP-1. Eur. J. Immunol. 27, 1091–1097.

Park, J.B., 2012. Synthesis, biological activities and bioavailability of moschamine, a safflomide-type phenylpropenoic acid amide found in Centaurea cyanus. Nat. Prod. Res. 26, 1465–1472.

Park, J.B., 2016. Finding potent sirt inhibitor in coffee: isolation, confirmation and synthesis of javamide-II (N-Caffeoyltryptophan) as Sirt1/2 inhibitor. PLoS One 17, e0150392.

Perkins, N.D., 2007. Integrating cell-signalling pathways with NF-kappaB and IKK function. Nat. Rev. Mol. Cell Biol. 8, 49–62.

Pessara, U., Koch, N., 1990. Tumor necrosis factor alpha regulates expression of the major histocompatibility complex class II-associated invariant chain by binding of an NF-kappaB-like factor to a promoter element. Mol. Cell. Biol. 10, 4146–4154.

Ruster, C., Wolf, G., 2008. The role of chemokines and chemokine receptors in diabetic nephropathy. Front. Biosci. 13, 944–955.

Saklatvala, J., 2004. The p38 MAP kinase pathway as a therapeutic target in inflammatory disease. Curr. Opin. Pharmacol. 4, 372–377.

Sheryanna, A., Bhangal, G., McDaid, J., Smith, J., Manning, A., Foxwell, B.M., Feldmann, M., Cook, H.T., Pusey, C.D., Tam, F.W., 2007. Inhibition of p38 mitogen-activated protein kinase is effective in the treatment of experimental crescentic glomerulonephritis and suppresses monocyte chemoattractant protein-1 but not IL-1beta or IL-6. J. Am. Soc. Nephrol. 18, 1167–1179.

Surh, Y.J., Chun, K.S., Cha, H.H., Han, S.S., Keum, Y.S., Park, K.K., Lee, S.S., 2001. Molecular mechanisms underlying chemopreventive activities of anti-inflammatory phytochemicals: down-regulation of COX-2 and iNOS through suppression of NF-kappa B activation. Mutat. Res. 1, 243–268.

Sutcliffe, A.M., Clarke, D.L., Bradbury, D.A., Corbett, L.M., Patel, J.A., Knox, A.J., 2009. Transcriptional regulation of monocyte chemotactic protein-1 release by endothelin-1 in human airway smooth muscle cells involves NF-kappaB and AP-1. Br. J. Pharmacol. 157, 436–450.

Tai, K., Iwasaki, H., Ikegaya, S., Ueda, T., 2013. Minocycline modulates cytokine and chemokine production in lipopolysaccharide-stimulated THP-1 monocytic cells by inhibiting IκB kinase α/β phosphorylation. Transl. Res. 161, 99–109.

Takahashi, Y., Perkins, S.N., Hursting, S.D., Wang, T.T., 2007. 17 beta-Estradiol differentially regulates androgen-responsive genes through estrogen receptor-beta and extracellular signal regulated kinase-dependent pathways in LNCaP human prostate cancer cells. Mol. Carcinog. 46, 117–129.

Takaishi, H., Taniguchi, T., Takahashi, A., Ishikawa, Y., Yokoyama, M., 2003. High glucose accelerates MCP-1 production via p38 MAPK in vascular endothelial cells. Biochem. Biophys. Res. Commun. 305, 122–128.

Vichai, V., Kirtikara, K., 2006. Sulforhodamine B colorimetric assay for cytotoxicity screening. Nat. Protoc. 1, 1112–1116.

Waas, W.F., Lo, H.H., Dalby, K.N., 2001. The kinetic mechanism of the dual phosphorylation of the ATF2 transcription factor by p38 mitogen-activated protein (MAP) kinase alpha. Implications for signal/response profiles of MAP kinase pathways. J. Biol. Chem. 276, 5676–5684.

Wong, C.K., Wang, C.B., Ip, W.K., Tian, Y.P., Lam, C.W., 2005. Role of p38 MAPK and NF-kB for chemokine release in coculture of human eosinophils and bronchial epithelial cells. Clin. Exp. Immunol. 139, 90–100.

Yang, C., Yu, L., Kong, L., Ma, R., Zhang, J., Zhu, Q., Zhu, J., Hao, D., 2014. Pyrroloquinoline quinone (PQQ) inhibits lipopolysaccharide induced inflammation in part via downregulated NF-κB and p38/JNK activation in microglial and attenuates microglia activation in lipopolysaccharide treatment mice. PLoS One 14, e109502.